

# Brillouin and Raman scattering from the acoustic vibrations of spherical particles with a size comparable to the wavelength of the light

M. Montagna\*

*Dipartimento di Fisica, CSMFO Group, Università di Trento, Via Sommarive 14, I-38100 Trento, Italy*  
(Received 20 September 2007; revised manuscript received 26 October 2007; published 23 January 2008)

The inelastic light scattering of the acoustic vibration of spherical nanoparticles has been studied within a continuum approximation, extending the previous models, valid for small particles, to the case of particle sizes comparable with the wavelength of the light. A mechanism appears, i.e. the polarizability modulation related to density changes, which is typical of Brillouin scattering and is negligible for small particles. Furthermore, the contribution of the polarizability modulation induced by the relative displacements of atoms, which produces the Raman scattering in small particles, strongly changes. Spheroidal modes other than the  $l=0$  and  $l=2$  ones, the only Raman active in small particles, contribute to both scattering mechanisms. As the size increases, higher  $l$  modes with higher  $n$ , the index that labels the radial wave vector, become important. In relatively large particles, the active  $(n, l, m)$  spheroidal modes are those with frequency close to that of the Brillouin active vibrations in the bulk material, i.e.,  $\omega^{nl} \approx qv_L$ , where  $\mathbf{q}$  is the exchanged wave vector of the light and  $v_L$  is the longitudinal sound velocity. Also torsional modes become active and produce depolarized light scattering with properties similar to those of transverse acoustic phonons.

DOI: 10.1103/PhysRevB.77.045418

PACS number(s): 78.30.-j, 78.35.+c, 63.22.-m, 62.30.+d

## I. INTRODUCTION

The acoustic vibrational dynamics of spheroidal clusters was studied by Lamb, who found the vibrational modes of a free homogeneous sphere.<sup>1</sup> The modes are classified as torsional and spheroidal ones, both labeled by three indices  $(nlm)$ , which describe the angular ( $lm$ ) and radial ( $n$ ) dependence of the displacement. On the basis of symmetry arguments, Duval showed that only the symmetric ( $l=0$ ) and quadrupolar ( $l=2$ ) spheroidal modes are Raman active.<sup>2</sup> This selection rule was confirmed by calculations of the strain components associated with the acoustic vibrations and by the analysis of their symmetry.<sup>3,4</sup> The  $l=0$  modes give a polarized [vertical-vertical (VV) parallel polarization in excitation and detection] Raman spectrum, whereas the  $l=2$  modes give depolarized spectra, allowing one to distinguish the nature of the vibrations by a comparison of the VV and horizontal-vertical (HV) (crossed polarizations) polarized spectra. There are no general rules that indicate either the relative intensity of the symmetric and quadrupolar Raman peaks, appearing in the VV spectrum, or the depolarization ratio  $DR_2 = I_{HV}/I_{VV}$  for the quadrupolar modes. These two quantities depend on the microscopic structure and on the physical mechanism of the phonon-photon interaction, which produces the polarizability modulation. These mechanisms are quite different for semiconductor, metal, and dielectric particles.<sup>4-6</sup> A lot of experimental data were well reproduced by assigning the observed low frequency peaks only to the symmetric ( $l=0$ ) and quadrupolar ( $l=2$ ) spheroidal vibrations.<sup>7-15</sup> The first modes ( $n=1$ ) of the sequences were usually observed, but weaker peaks, attributed to modes with  $n > 1$ , were also observed in some systems.<sup>10,12-14</sup> Their intensities were well reproduced by calculations based on a strain model.<sup>3</sup>

However, all of the above cited experiments were performed on systems formed by very small particles of size  $D \ll \lambda$  or  $qD \ll 1$ , where  $\lambda$  is the wavelength and  $q$  is the

exchanged wave vector of light. In fact, the theoretical results were derived in the hypothesis that the fields, scattered by different polarizable units within the particle, are all in phase,  $qD \ll 1$ .

Recently, light scattering experiments from particles with sizes of hundreds of nanometers have been performed.<sup>16-19</sup> The particles were made up of sol-gel derived silica, polystyrene or polymethyl methacrylate, aggregated to form three dimensional photonic crystals. The low frequency spectra of these systems, and those relative to a single particle,<sup>20</sup> exhibit many peaks with comparable intensities. The peaks were attributed to the spheroidal  $(n, l)$  acoustic vibrations confined in a single sphere. Modes with  $l=0, 2, 4, 6$  were observed. The assignments were based on a best fit of the frequencies calculated by the Lamb model, to the observed ones. In these fits, the sound velocities were used as free parameters. Up to 21 vibrational modes, with also high values of both  $n$  and  $l$ , were observed for polystyrene spheres.<sup>19</sup> No selection rule for  $n$  and  $l$  was considered based on the idea that for  $qD \sim 1$ , all the theoretical results need a revision. Unfortunately, the strong Mie scattering of the light that occurs for  $\lambda \sim D$  prevents the measurement of polarized spectra because the polarization is lost in a multiple scattering process. Furthermore, multiple scattering strongly reduces the information on the  $q$  dependence of the spectra. In fact, measurements performed in a backscattering configuration contain contributions from all exchanged wave vectors ( $0 < q < 4\pi n_r / \lambda_0$ , where  $n_r$  is the refractive index and  $\lambda_0$  is the wavelength of the light in vacuum). Polarized  $q$ -dependent spectra were taken by immersing the particles in a liquid with a matched refractive index.<sup>17</sup> The strong depolarized scattering due to the relaxation of the liquid, the interaction between localized modes of the particles and the phonons of the liquid, which produces line broadening, as well as the interaction among the particles gave interesting physical results, but not a direct information on the single particle spectra.

Some assignments, as those of Table I in Ref. 19 only based on the calculated frequencies of the modes, could be not correct, especially for high frequency modes, which become much denser as the angular  $l$  and radial  $n$  indices increase. It is evident that a theoretical analysis of the expected Raman activity of the different modes would strongly help. The aim of the present work is therefore to study how the selection rules, valid for small particles ( $qD \ll 1$ ), evolve as  $qD$  increases.

## II. BRILLOUIN AND RAMAN SCATTERING

A method for calculating the low frequency Raman spectrum of dielectric nanoparticles has been developed in Refs. 3 and 6.

The spectral density of the scattered light is given by<sup>21</sup>

$$I_{\alpha\beta}(\mathbf{q}, \omega) \propto \int dt e^{-i\omega t} \langle \delta\epsilon_{\alpha\beta}^*(\mathbf{q}, 0) \delta\epsilon_{\alpha\beta}(\mathbf{q}, t) \rangle, \quad (1)$$

where  $\alpha$  and  $\beta$  are the direction of polarization of the incident and scattered photons, respectively, and  $\hbar\omega = \hbar\omega_i - \hbar\omega_s$  and  $\mathbf{q} = \mathbf{k}_i - \mathbf{k}_s$  are the exchanged energy and wave vector, respectively. The fluctuations of the dielectric constant can be described in terms of the space Fourier transform of the macroscopic polarizability density tensor  $P_{\alpha\beta}(\mathbf{r}, t)$ ,

$$\delta\epsilon_{\alpha\beta}(\mathbf{q}, t) \propto \int d\mathbf{r} e^{-i\mathbf{q}\cdot\mathbf{r}(t)} P_{\alpha\beta}(\mathbf{r}, t) = \sum_i e^{-i\mathbf{q}\cdot\mathbf{r}^i(t)} \pi_{\alpha\beta}^i(t), \quad (2)$$

which in atomic or molecular systems can be described microscopically by using the effective microscopic polarizability tensor  $\pi_{\alpha\beta}^i(t)$  of the  $i$ th scatterer at position  $\mathbf{r}^i(t)$ ,

$$\mathbf{r}^i(t) = \mathbf{x}^i + \mathbf{u}^i(t), \quad (3)$$

where  $\mathbf{u}^i(t)$  is the displacement from the equilibrium position  $\mathbf{x}^i$ .

$\pi_{\alpha\beta}^i(t)$  can be expanded in power series of the displacements  $\mathbf{u}^i$ , and  $\mathbf{u}^i$  can be expressed in terms of the vibrational eigenvectors  $\mathbf{e}(i, p)$ , whose frequencies are  $\omega_p$ ,

$$\pi_{\alpha\beta}^i(t) = \pi_{\alpha\beta}^i + Q_{\alpha\beta}^i, \quad (4)$$

with

$$Q_{\alpha\beta}^i = \sum_j \sum_\gamma \frac{\partial \pi_{\alpha\beta}^i}{\partial u_\gamma^j} [e_{\gamma(j,p)} - e_{\gamma(i,p)}]. \quad (5)$$

$\pi_{\alpha\beta}^i$  is the bare polarizability of the  $i$ th unit, and its derivatives with respect to the displacements of the surrounding atoms are calculated at the equilibrium position  $\mathbf{x}^i$ .

The contribution of the  $p$ th mode, with frequency  $\omega_p$ , to the Stokes part of the spectrum can be put in the form<sup>22</sup>

$$\begin{aligned} I_{\alpha\beta}^p(\mathbf{q}) &\propto \frac{n(\omega^p) + 1}{\omega^p} \left| \sum_i e^{-i\mathbf{q}\cdot\mathbf{x}^i} [-i\mathbf{q} \cdot \mathbf{e}(i, p) \pi_{\alpha\beta}^i + Q_{\alpha\beta}^i] \right|^2 \\ &= \frac{n(\omega^p) + 1}{\omega^p} C_{\alpha\beta}(\omega^p), \end{aligned} \quad (6)$$

where  $n(\omega, T)$  is the Bose-Einstein factor and  $C_{\alpha\beta}(\omega_p)$  is the mode-radiation coupling coefficient.

The first term,  $-i\sum_i \pi_{\alpha\beta}^i e^{-i\mathbf{q}\cdot\mathbf{x}^i} \mathbf{q} \cdot \mathbf{e}(i, p)$ , describes the polarization fluctuations due to the displacement of the units from their equilibrium position: The density of microscopic polarization units, atoms, ions, and bonds is modulated by the acoustic vibrations. Inelastic neutron scattering and, usually, most of the polarized Brillouin scatterings are due to these density fluctuations caused by longitudinal acoustic phonons. In the following, we will refer to it as the Brillouin term.

The second term,  $\sum_i e^{-i\mathbf{q}\cdot\mathbf{x}^i} Q_{\alpha\beta}^i$ , is due to two kinds of induced effects: (i) The local field changes due to the motion of the surrounding dipoles [dipole induced dipoles (DID)]. (ii) The electronic polarizability changes with the change of the atomic distances [bond polarization (BP)]. The induced effects contribute to the polarized Brillouin peak due to longitudinal phonons and cause the depolarized Brillouin peak due to transversal phonons and the disorder induced low frequency Raman scattering in glasses or disordered crystals. In the following, we will refer to this term as the Raman term.

The Brillouin term was not considered in Ref. 3. In fact, if the particle size  $D$  is much smaller than the wavelength of the exciting light, the mechanism of scattering due to density fluctuations is not active. For spherical particles ( $D=2R$ ), we will find a  $(qR)^4$  dependence of the Brillouin intensity, for small  $qR$  values. Therefore, only the Raman term is active for small particles ( $qR \ll 1$ ). All polarization units are excited in phase, and the particle behaves as a molecule, which can be described by an effective polarizability and by its derivatives with respect to the coordinates of the normal modes. The important difference with the Brillouin scattering is that no  $q$  dependence is present, so that isotropic scattering is observed instead of the Bragg-like scattering, typical of systems that extend over many wavelengths.

For particles with a size comparable to the wavelength of the light, both the Brillouin and Raman terms will be important. We will treat the two contributions separately, but note that the two terms interfere: The intensity at a given frequency and  $\mathbf{q}$  is proportional to the square of the sum of the field amplitudes given by the two mechanisms, as Eq. (6) clearly shows.

## III. BRILLOUIN SCATTERING FROM THE SPHEROIDAL MODES

In a continuum approximation, we can use the equilibrium macroscopic polarizability density tensor  $P_{\alpha\beta}(\mathbf{x})$  instead of  $\pi_{\alpha\beta}^i$  and transform the sum into a space integral. Furthermore, if the material is homogeneous and isotropic, we will have

$$P_{\alpha\beta}(\mathbf{x}) = P \delta_{\alpha\beta}, \quad (7)$$

where  $P$  is the macroscopic polarizability density. This indicates that the Brillouin term due to the density fluctuations produces only polarized scattering from the acoustic vibration of the nanoparticles, as the corresponding term does for the usual case of phonons.

The amplitude of the Brillouin scattered field by the  $p$ th mode will be

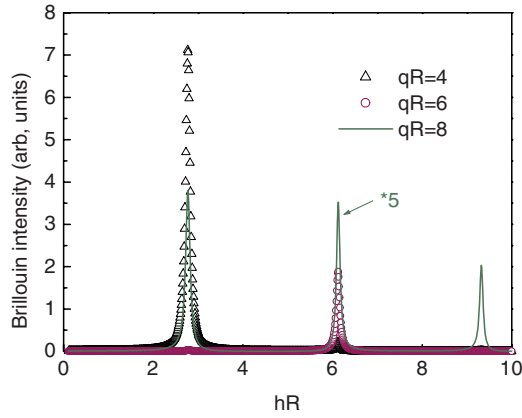


FIG. 1. (Color online) Contribution of the Brillouin term to the spectra from the symmetric spheroidal vibrations, for  $qR=4$  (open triangles),  $qR=6$  (open circles), and  $qR=8$  (solid line, multiplied by a factor of 5).

$$B_{\alpha\alpha}^B(p, q) = C_{\alpha\alpha}^B(p, q)^{1/2} = -iqP \int_V e^{-iqz} e_z^p(\mathbf{x}) d\mathbf{x}, \quad (8)$$

having chosen the  $z$  axis along  $\mathbf{q}$ .

We will discuss in detail the simple case of the symmetric spheroidal modes. The radial displacement,  $e(r)$ , of the  $l=0$  modes is obtained from the symmetric potential:

$$\phi^0(h, r) = A(h)h \frac{\sin hr}{hr}, \quad (9)$$

$$e^0(h, r) = \frac{A(h)h^2}{hr} \left( \cos hr - \frac{\sin hr}{hr} \right), \quad (10)$$

where  $h$  is the radial wave vector and the amplitude  $A(h)$  is determined by normalization and boundary conditions. For a free particle, a discrete set of wave vectors  $h_n$  and relative frequencies  $\omega_n^0 = h_n v_L$  is obtained for stress-free boundary conditions at the sphere surface. For particles embedded in a matrix, the displacement extends into the external material and the discrete set of modes become a continuum.  $A(h)$  is obtained by normalization and continuity of the displacement and stress at the particle surface.

By inserting the  $l=0$  displacement of Eq. (10) in Eq. (8), we obtain

$$B_{\alpha\alpha}^B(0, h, q) = P4\pi h \left[ \frac{h}{h^2 - q^2} \cos qR \sin hR + \frac{q}{q^2 - h^2} \cos hR \sin qR - \frac{1}{qhR} \sin hR \sin qR \right]. \quad (11)$$

The inelastic light scattering intensity, obtained by Eq. (6) with the above scattering amplitude,  $B_{\alpha\alpha}^B(0, h, q)$ , is shown in Fig. 1 as a function of the adimensional radial wave vector  $hR$  for some  $qR$  values. The calculation is relative to a system with  $v_L/v_T=2$ . For numerical and graphical practical

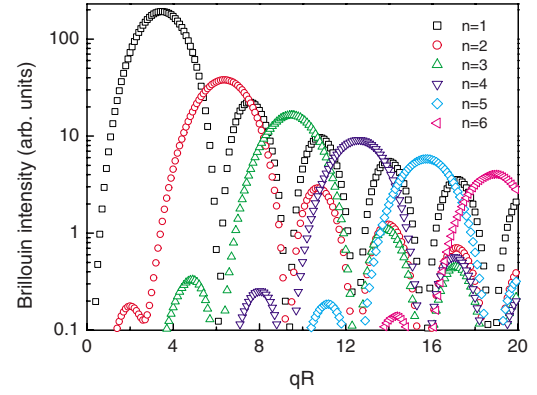


FIG. 2. (Color online)  $q$  dependence of the intensities given by the Brillouin term for the first six modes in the sequence of the symmetric spheroidal vibrations.

reasons, instead of a free particle, a quasi-free sphere in a soft medium has been considered. The sound velocities and the density of the medium were  $1/4$  of those of the particle. The spectrum calculated for  $qR=4$  shows an intense  $n=1$  peak at  $hR=2.8$ , with a weaker  $n=2$  peak at  $hR=6.1$ , the intensity of the higher  $n$  modes being negligible. For  $qR=6$ , an intense  $n=2$  peak dominates the spectrum. For  $qR=8$ , the  $n=1, 2, 3$  peaks have comparable intensities. The results of these three examples are extended in Fig. 2, which shows the intensities of the six lowest frequency peaks of the  $l=0$  sequence, as a function of  $qR$ . Spectra as those of Fig. 1 were calculated for many  $q$  values in the range  $0 < qR < 20$ . The intensities of the  $(n, 0)$  modes were obtained by calculating the areas of the peaks, which are centered at frequencies more or less independent of  $q$ , as Fig 1 shows. Resonances appear at  $h=q$ . Besides the presence of the  $(q-h)$  denominator, the resonances are broad, with a width in  $hR$  of the order of  $\pi$ , since the term  $\frac{\sin(q-h)R}{(q-h)R}$  appears in Eq. (11) for  $h \approx q$ . For  $qR < 1$ , only the  $n=1$  mode appears to be active with an intensity that initially grows as  $q^4$  and reaches a maximum at  $qR \sim 3.5$ , to be compared with the wave vector of the  $n=1$  mode,  $h_1 R = 2.8$ . For a backscattering geometry, for  $\lambda \sim 514.5$  nm, and for  $n_r \sim 1.5$ , this corresponds to particles with a size  $2R = (h_1 R) \lambda / 2\pi n_r \sim 150$  nm. Only the second mode is expected for a particle size of about 300 nm, only the third mode for a size of about 450 nm, and so on. Only one or two peaks dominate the spectrum at any  $q$  value, those with  $h$  values near to  $q$  (see also Fig. 1), but the  $l=0$  mode periodically appears important even for high  $qR$  values.

This detailed study for the symmetric mode cannot be easily extended to the  $l \neq 0$  vibrations. Instead, two different approaches will be used. The first approach considers, for any  $q$  value, the angular symmetry of the scattered field,  $e^{-iqz} e_z^p(\mathbf{x})$ : Only terms transforming as  $Y_{00}$  can possibly contribute to the angular part of the integral in Eq. (8), which gives the total scattered field. The angular dependence of the displacement field of the spheroidal modes,  $e_{\alpha}^{nlm}$ , is given by<sup>23</sup>

$$e_{\alpha}^{nlm} = A(r)x_{\alpha}Y_{lm}(\theta, \phi) + B(r)\frac{\partial r^l Y_{lm}(\theta, \phi)}{\partial x_{\alpha}}, \quad (12)$$

where  $A(r)$  and  $B(r)$  are radial functions typical of each mode with frequency  $\omega_{nl}$ . The first term in the sum transforms as  $Y_{l+1, m'}$ , the second, not present for  $l=0$ , as  $Y_{l-1, m'}$ .

The exponential can be expanded as

$$e^{-iqz} = \sum_s \frac{1}{s!} (-iqr \cos \theta)^s = \sum_{l'} a_{l'}(qr) P_{l'}(\cos \theta), \quad (13)$$

where the angular dependence has been evidenced by introducing the Legendre polynomials. Note that there is no direct correspondence between terms with  $s=l'$  in the two sums since  $P_{l'}(\cos \theta)$  contains terms in  $(\cos \theta)^{l'}$ ,  $(\cos \theta)^{l'-2}$ , ... However, the  $(qr \cos \theta)^{l'}$  term of the development of the exponential is needed for having an  $a_{l'} \neq 0$ . By combining the symmetry properties of the quantities in Eqs. (12) and (13), we find the selection rule  $l'=l \pm 1$ . Therefore, for low  $qR$ , only modes with low  $l$  values will be active and, as  $qR$  increases, vibrations with much higher  $l$  modes will become active.

The second approach considers the evolution of Brillouin spectrum starting from a large sphere and progressively decreasing its size. In a macroscopic sphere, Brillouin scattering will be produced by longitudinal acoustical phonons at frequencies given by  $\omega = qv_L$ ; by decreasing the size, the discrete sequences  $(n, l)$  will appear.<sup>24</sup> However, the description of the acoustic vibrations in terms of longitudinal plane waves,  $\mathbf{e}_q$ , or waves of the sphere,  $\mathbf{e}^{plm}$ , must be equivalent. This is true for large particles and for high vibrational frequencies when the modes are very dense, so that the frequency difference between pairs of successive vibrational modes of the sphere is smaller than the homogeneous linewidth due to anharmonicity or to the interaction of the sphere with a surrounding matrix. An  $(n, l, m)$  mode can be described as the superposition of acoustic phonons and vice versa. The amplitudes of the terms in the developments will be proportional to  $\int_V e^{-ik \cdot r} \mathbf{e}^p(\mathbf{x}) d\mathbf{x}$ . This is the same quantity that appears in the amplitude of the scattered Brillouin field of Eq. (8), but now the phonon wave vector  $\mathbf{k}$  appears instead of the exchanged wave vector  $\mathbf{q}$ . Therefore, only  $(n, l, m)$  modes with frequencies close to  $qv_L$  will contribute to the Brillouin spectrum. A possible picture is that the photon is inelastically scattered by the dynamical Bragg grating associated with the mode of the sphere. Both radial and angular oscillations produce the grating, whose pitch decreases as  $n$  and  $l$  increase. The maximum scattering efficiency will occur for the best matching between the photon wavelength (in fact, the relevant quantity is  $\mathbf{q}$ ) and the pitch of this spherical grating. This occurs when the  $(n, l, m)$  vibration has a frequency close to  $qv_L$ . The efficiency of the grating is smaller than that of the grating produced by the plane wave of a phonon, and broader  $q$  resonances, like those shown in Fig. 2, will appear. This result, obtained for large particles ( $qR \gg 1$ ), should be valid also for medium-sized particles ( $qR \sim 1$ ). Figure 2, relative to the  $l=0$  modes, confirms this

conjecture: The resonance at  $h=q$  selects modes with frequencies  $\omega^{n0} = h_n v_L$  close to  $qv_L$ .

#### IV. RAMAN SCATTERING FROM SPHEROIDAL MODES

The scattering amplitude of the  $p$ th mode, due to the induced term  $Q_{\alpha\beta}$ , is given by

$$B_{\alpha\beta}^R(p, \mathbf{q}) = \sum_{\gamma\delta} \sum_i A_{\alpha\beta\gamma\delta}(\mathbf{x}^i) \frac{\partial e_{\gamma}(\mathbf{x}^i, p)}{\partial x_{\delta}} \exp(-i\mathbf{q} \cdot \mathbf{x}^i), \quad (14)$$

where the  $\frac{\partial e_{\gamma}(\mathbf{x}^i, p)}{\partial x_{\delta}}$  are related to the strain components at  $\mathbf{x}^i$  produced by the normal mode  $\mathbf{e}(i, p)$ . The  $A_{\alpha\beta\gamma\delta}$  coefficients are local quantities to be calculated at the equilibrium position of the  $i$ th unit and do not depend on the vibrations. Equation (14) has been modified by the addition of the term  $\exp(-i\mathbf{q} \cdot \mathbf{x}^i)$ , not present in Refs. 3 and 6.

For crystalline particles, by neglecting the size dependence of the  $A_{\alpha\beta\gamma\delta}$ , i.e., by neglecting surface effects and by converting the sum on the point scatterers into an integral on the volume of the sphere in a continuum description of the vibrational modes, we obtain

$$B_{\alpha\beta}^R(p, \mathbf{q}) = N \sum_{k\gamma\delta} A_{\alpha\beta\gamma\delta}^k \int \frac{\partial e_{\gamma}(\mathbf{x}, p)}{\partial x_{\delta}} \exp(-i\mathbf{q} \cdot \mathbf{x}) d\mathbf{x}, \quad (15)$$

where  $N$  is the number of unitary cells in the crystalline sphere and the sum over  $k$  runs over the atoms (ions) in the unit cell. In amorphous particles, instead of a sum on the atoms, averaged  $A_{\alpha\beta\gamma\delta}$  will be needed. For depolarized scattering, the quantity  $A_{\alpha\beta\alpha\beta}$  ( $\alpha \neq \beta$ ) is proportional to the  $p_{44}$  elasto-optical constant. On the contrary,  $p_{11}$  and  $p_{12}$  used to determine the intensities of the longitudinal peak of Brillouin scattering, in addition to the contribution from the  $A_{\alpha\alpha\alpha\alpha}$  and  $A_{\alpha\alpha\beta\beta}$ , have a main contribution from the Brillouin term discussed in the previous section.

In this way, the problem of calculating the Raman intensities is reduced to the calculation of the dynamical quantities,

$$E_{\gamma\delta}(\mathbf{q}) = \int \varepsilon_{\gamma\delta}(\mathbf{x}, p) \exp(-i\mathbf{q} \cdot \mathbf{x}) d\mathbf{x}, \quad (16)$$

where  $\varepsilon_{\gamma\delta}(\mathbf{x}, p) = \frac{1}{2} \left[ \frac{\partial e_{\gamma}(\mathbf{x}, p)}{\partial x_{\delta}} + \frac{\partial e_{\delta}(\mathbf{x}, p)}{\partial x_{\gamma}} \right]$  are the strain components produced by the  $p$ th vibrational mode.

The first question to answer is the  $q$  dependence of the Raman intensity of the modes in an  $n$  sequence for defined  $l$ . The  $l=0$  sequence of symmetric modes will be studied in detail since an analytical solution exists in this simple case.

The spatial derivatives of the displacement are

$$\frac{\partial e_{\gamma}}{\partial x_{\delta}} = F_{\gamma\delta}(r) + G(r)x_{\gamma}x_{\delta}, \quad (17)$$

with

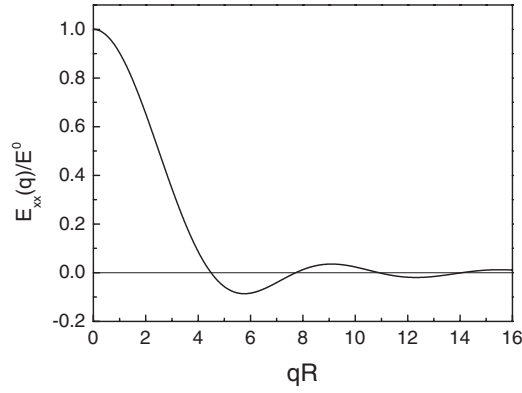


FIG. 3.  $q$  dependence of  $E_{xx}$  (see text) for the  $l=0$  symmetric spheroidal modes.

$$F_{\gamma\delta}(r) = \frac{Ah^3}{(hr)^2} \left( \cos hr - \frac{\sin hr}{hr} \right) \delta_{\gamma\delta} \quad (18)$$

and

$$G(r) = \frac{Ah^5}{(hr)^5} [-3hr \cos hr + 3 \sin hr - (hr)^2 \sin hr]. \quad (19)$$

The dynamical quantities  $E_{\gamma\delta}(\mathbf{q})$  are obtained by the volume integration, in spherical coordinates, of Eq. (16). By taking the  $z$  axis along  $\mathbf{q}$ , the interesting quantities are  $E_{xx}(\mathbf{q})=E_{yy}(\mathbf{q})$  and  $E_{zz}(\mathbf{q})$ , with  $E_{\gamma\delta}(\mathbf{q})=0$  for  $\gamma \neq \delta$ , as shown by Eqs. (17)–(19), because integrals of odd functions appear in this case. This shows that the Raman scattering from the symmetric modes remains polarized even at  $\mathbf{q} \neq 0$ . The following results have been obtained:

$$E_{xx}(q, h) = E_{\alpha\alpha}(0, h) \frac{3 \left( \frac{\sin qR}{qR} - \cos qR \right)}{(qR)^2}, \quad (20)$$

where

$$E_{\alpha\alpha}(0, h) = \frac{4}{3} \pi A(h) h R \left( \cos hR - \frac{\sin hR}{hR} \right) = E^0 \quad (21)$$

is the  $q=0$  strain integral.<sup>3</sup> The factor  $E_{xx}(q, h)/E^0$ , shown in Fig. 3, does not depend on the radial wave vector  $h$  so that the relative intensity of all modes of the sequence remains the same.

More interesting is the result of the calculation of  $E_{zz}(q, h)$ , whose expression, quite long, is not reported. Its  $h$  dependence changes with  $q$ , as shown in Fig. 4. For  $q=0$ , the (modulus of the) strain integral is more or less the same for all the  $n$  values. This is due to an effect of compensation between the linear increase of the local strain with the radial wave vector and the increase of the destructive interference among regions having a local strain of opposite sign. In fact, the displacement field of the  $n$ th mode has  $n-1$  radial nodes and the corresponding radial strain  $n$  nodes. The observed intensity decrease, as  $n$  increases, is therefore almost completely due to the thermal averages involving phonon popu-

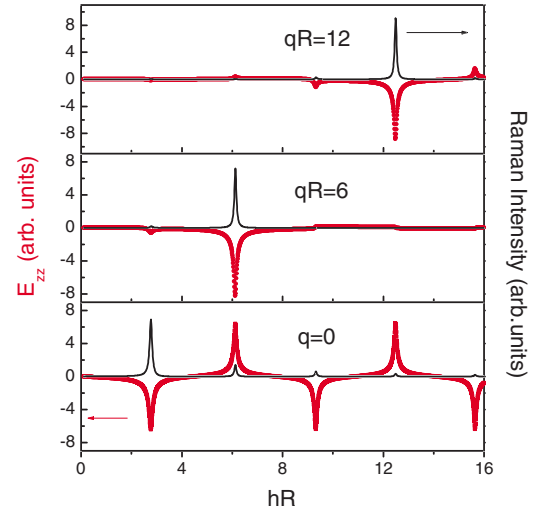


FIG. 4. (Color online)  $hR$  dependence of the  $zz$  strain integrals  $E_{zz}$  and of  $E_{zz}^2/(hR)^2$ , a quantity related to the Raman intensity (see text), for the symmetric spheroidal vibrations and for  $qR=0, 6, 12$ .

lations and 1-phonon transition rates, not to differences in the phonon-photon coupling coefficients,  $C_{\alpha\alpha}^{0,n}$ . The shape of the Raman spectrum is obtained by squaring the strain integral and dividing by the square of the frequency since  $[n(\omega) + 1]/\omega \propto 1/\omega^2$  for  $kT \gg \hbar\omega$ . This is true only for  $q=0$  because  $E_{xx}(0, h)=E_{yy}(0, h)=E_{zz}(0, h)$ , as it will be clearer in the following. As  $qR$  increases, the scattering amplitude of the lowest frequency mode ( $n=1$ ) decreases and modes with  $n > 1$  become dominant. In the example of Fig. 4, the  $n=2$  mode is dominant at  $qR=6$ , and the  $n=4$  at  $qR=12$ . The scale of  $E_{zz}$  is arbitrary but the same for the different  $qR$  values. Modes with different  $n$  values reach a maximum Raman activity at different  $qR$  values, but the scattered fields have comparable amplitudes at the maximum. This is clearer in Fig. 5, which shows the square of the  $zz$  strain integrals of Eq. (16), integrated on the frequency ranges covered by the first five  $l=0$  modes. Broad resonances at  $q=h_n$  appear, similar to those already observed for the Brillouin scattering mechanism of the previous section.

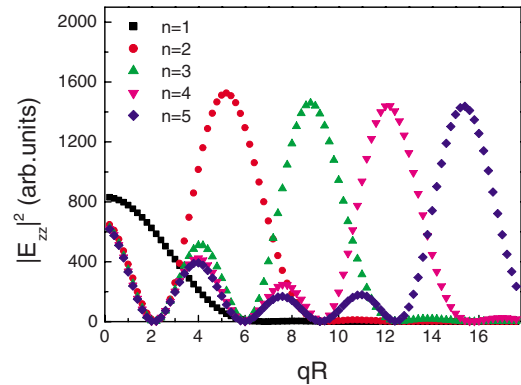


FIG. 5. (Color online)  $q$  dependence of the square of the  $zz$  strain integral  $|E_{zz}|^2$  for the first five modes in the sequence of the symmetric spheroidal vibrations.

In order to obtain the Raman spectrum from the knowledge of the  $E_{\alpha\alpha}$  strain integrals, we need to define the geometry of the experiment and to know the microscopic mechanisms that modulate the polarizability. For example, in the backscattering configuration that is used in most Brillouin scattering experiments, the incoming and scattered light are both parallel to  $\mathbf{q}$  (along  $\hat{\mathbf{z}}$ ), and taking  $\hat{\mathbf{x}}$  parallel to the polarization axis, we obtain

$$B_{xx}^R = A_{xxxx}E_{xx} + A_{xyxy}E_{yy} + A_{xxzz}E_{zz}. \quad (22)$$

The  $E_{\alpha\alpha}$  quantities have been calculated above as a function of the frequency and of the wave vector, but the  $A_{\alpha\alpha\beta\beta}$  quantities, which measure the fluctuations of the polarizability induced by the vibrational mode, are also needed. In Ref. 6, it has been shown that in dielectric materials we can consider the DID and/or BP scattering mechanisms. For DID, the relation  $A_{xxxx} = -2A_{xyxy} = -2A_{xxzz}$  holds; for BP, the relation is  $A_{xxxx} = A_{xyxy} = A_{xxzz}$ . The different dependence of  $E_{xx} = E_{yy}$  and  $E_{zz}$  on frequency and exchanged wave vector, makes the shape of the Raman spectrum dependent on the scattering mechanism. Furthermore, the intensity of the scattered light is not the sum of the intensities given by the Brillouin and Raman terms. The two terms interfere and the coupling coefficient of the  $p$ th mode, in general, will be given by

$$C_{\alpha\alpha}(p, q) = |B_{\alpha\alpha}^B(p, q) + B_{\alpha\alpha}^R(p, q)|^2. \quad (23)$$

A qualitative discussion of the effect of  $qR \neq 0$  on the  $l > 0$  spheroidal modes can follow the two approaches used for Brillouin scattering. Instead of the symmetry of the displacement field, for Raman scattering we must consider the symmetry of the strain components. Taking the derivative of Eq. (12), we obtain

$$\begin{aligned} \frac{\partial e_{\alpha}^{nlm}}{\partial x_{\beta}} &= [A'(r)x_{\alpha}x_{\beta} + B'(r)\delta_{\alpha\beta}]r^l Y_{lm}(\theta, \phi) \\ &+ C'(r)x_{\beta} \frac{\partial r^l Y_{lm}(\theta, \phi)}{\partial x_{\alpha}} + D'(r)x_{\alpha} \frac{\partial r^l Y_{lm}(\theta, \phi)}{\partial x_{\beta}} \\ &+ E'(r) \frac{\partial r^l Y_{lm}(\theta, \phi)}{\partial x_{\alpha} \partial x_{\beta}}, \end{aligned} \quad (24)$$

where  $A', B', C', \dots$  are radial functions typical of each mode with frequency  $\omega^{nl}$ . The terms in the sum transform as  $Y_{lm'}$  or  $Y_{l-2, m'}$  or  $Y_{l+2, m'}$ . Therefore, for  $q=0$ , only the  $l=0$  and  $l=2$  spheroidal modes can contribute to Raman scattering. The same arguments used in the section of the Brillouin scattering indicate that, as  $q$  increases, modes with progressively higher  $l$  symmetry will become Raman active.

As for the second approach, we observe that in a macroscopic sample, the induced (Raman) terms produce the depolarized transverse peak at the frequency  $\omega_T = qv_T$  and also contribute to the polarized longitudinal peak at the frequency  $\omega_L = qv_L$ . Therefore, two sets of acoustic modes of a macroscopic sphere are active, whereas in the Brillouin term only the modes resonant with the longitudinal phonons were active. The discussion and the conjectures proposed for the

case of the Brillouin term can be extended to the present case. In fact, the dynamical grating of the strain and that of the displacement field are closely related.

Saviot and Murray showed that the spheroidal modes can be grouped into two categories: primarily longitudinal and primarily transverse.<sup>25</sup> They also showed that modes of both natures are present in a sequence  $(n, l)$  with fixed  $l > 0$ , whereas for  $l=0$ , all modes have a dominant longitudinal character. The longitudinal or transverse nature of a mode will determine its contribution to the VV Raman and Brillouin terms or to the HV Raman term, respectively. Furthermore, the study of Saviot and Murray evidences the sensitivity of the displacement field and the strain tensor to the ratio of the transverse and longitudinal sound velocities, indicating that a specific calculation of the Brillouin-Raman spectra, devoted to a given system, is needed.

## V. TORSIONAL VIBRATIONS

So far, we did not consider the torsional vibrations. Their vibrational modes are described by the displacement field,

$$e_{\gamma}^{nlm} = A\psi_n(\kappa r) \left[ x_{\alpha} \frac{\partial r^l Y_{lm}(\theta, \phi)}{\partial x_{\beta}} - x_{\beta} \frac{\partial r^l Y_{lm}(\theta, \phi)}{\partial x_{\alpha}} \right], \quad (25)$$

with  $\alpha, \beta$ , and  $\gamma$  in cyclic order, where  $\kappa$  is the radial wave vector and  $\psi_n(x) = \left(\frac{1}{x} \frac{d}{dx}\right)^n \left(\frac{\sin x}{x}\right)$ .<sup>23</sup>

These are pure torsional modes, which do not produce dilatation, but only shear, and have no radial displacement. The displacement at any point is directed at a right angle to the radius drawn from the center of the sphere. Equation (8) shows that none of these modes, for any direction of  $\mathbf{q}$ , can contribute to the Brillouin term. In fact, for Brillouin scattering, the relevant displacement is that parallel to  $\mathbf{q}$ , which has its typical rotatory symmetry in a plane normal to its direction. This is in agreement with the general property that a pure shear vibration, in the absence of density changes, cannot produce Brillouin scattering by the Brillouin term, but only the transverse peak at  $\omega = qv_T$  by induced (Raman) terms.

The angular symmetries of the strain components are obtained by taking the derivative of the displacements,

$$\begin{aligned} \frac{\partial e_{\gamma}^{nlm}}{\partial x_{\delta}} &= A(r) \left[ \frac{\partial r^l Y_{lm}}{\partial x_{\beta}} \delta_{\alpha\delta} - \frac{\partial r^l Y_{lm}}{\partial x_{\alpha}} \delta_{\beta\delta} \right] \\ &+ B(r) \left[ \frac{\partial r^l Y_{lm}(\theta, \phi)}{\partial x_{\beta}} x_{\alpha} x_{\delta} - \frac{\partial r^l Y_{lm}}{\partial x_{\alpha}} x_{\beta} x_{\delta} \right] \\ &+ C(r) \left[ \frac{\partial^2 r^l Y_{lm}}{\partial x_{\beta} \partial x_{\delta}} x_{\alpha} - \frac{\partial^2 r^l Y_{lm}}{\partial x_{\alpha} \partial x_{\delta}} x_{\beta} \right]. \end{aligned} \quad (26)$$

From the point of view of angular symmetry, the  $l=1$  and  $l=3$  terms would be Raman active even for  $q=0$ , but this is not the case, as can be shown by taking the strain integral of Eq. (12).

The displacement of the  $x$  component of the  $l=1$  mode is

$$e_x^{m1x} = 0, \quad e_y^{m1x} = A\psi_1(\kappa r)z, \quad e_z^{m1x} = -A\psi_1(\kappa r)y. \quad (27)$$

The displacements of the other two components can be obtained by cyclic changes of the indices. These rotatory vibrations are pure rotations of concentric spheres around a symmetry axis, the  $x$  axis for the component of Eq. (27), by a (small) quantity proportional to  $\psi_1(\kappa r)$ . Taking the derivatives of these quantities, the following equations are found for the nonzero components of the strain tensor:

$$\begin{aligned} \varepsilon_{yy}^{m1x} &= A(\kappa_n r)\psi_1'(\kappa_n r)\frac{\kappa xy}{r} = -\varepsilon_{zz}^{m1x}, \\ \varepsilon_{xy}^{m1x} &= A(\kappa_n r)\psi_1'(\kappa_n r)\frac{\kappa zx}{2r}, \\ \varepsilon_{zx}^{m1x} &= -A(\kappa_n r)\psi_1'(\kappa_n r)\frac{\kappa xy}{2r}, \\ \varepsilon_{yz}^{m1x} &= A(\kappa_n r)\psi_1'(\kappa_n r)\frac{z^2 - y^2}{2r}. \end{aligned} \quad (28)$$

We can observe that the  $\mathbf{q}=0$  strain integrals,  $\int \varepsilon_{\alpha\beta} d\mathbf{x}$ , are all zero, the first three ones because of the odd symmetry of  $x$ ,  $y$ , and  $z$ , the fourth one because the average values of  $z^2$  and  $y^2$  on the sphere are equal. By similar arguments, it has been recently shown that also the  $l=3$  mode is not Raman active at  $\mathbf{q}=0$ .<sup>26</sup> For  $\mathbf{q} \neq 0$ , assumed along the  $z$  axis, we have to take the strain integral of Eq. (16). Symmetry considerations on the  $\varepsilon_{\alpha\beta}(\mathbf{x})\exp(iqz)$  quantity show that the  $E_{yy}(\mathbf{q})=E_{zz}(\mathbf{q})=E_{xy}(\mathbf{q})=E_{zx}(\mathbf{q})=0$ . The only nonzero strain integral is  $E_{yz}(\mathbf{q})$ . It has not a simple analytical form and needs numerical calculation. It will contribute only to the depolarized spectrum, but not in the backscattering geometry, which would need a strain integral  $E_{xy}(\mathbf{q}) \neq 0$  for  $\mathbf{q} = q\hat{z}$ . This property is the same that holds for the normal Brillouin scattering from transverse phonons, and confirms the close relation between torsional vibrations and transverse phonons. The arguments used in the previous sections indicate that  $(tnlm)$  modes nearly resonant with  $qv_T$  will have an important activity and therefore that the relevant  $n$  and  $l$  values increase with  $q$ .

## VI. COMPARISON WITH THE AVAILABLE EXPERIMENTAL RESULTS

In the Brillouin experiments by Li *et al.*,<sup>20</sup> single particles and particle aggregates of porous silica were studied. The particle size was in the range  $262 < 2R < 515$  nm. Vibrational modes with  $(n,l)=(1,2),(1,0),(2,2),(1,4),(1,6)$ , in increasing order of frequency, were observed in a range between about 5 and 20 GHz. For a backscattering experiment with the 514.5 nm laser line, assuming that the refractive index is  $n_r \approx 1.4$ , an exchanged  $q \approx 0.034$  nm<sup>-1</sup> can be estimated. The  $qR$  values corresponding to  $262 < 2R < 515$  nm can be estimated as  $4.4 < qR < 8.7$ , and for  $v_L \approx 4$  km/s, a resonance frequency of about 14 GHz is obtained. For the  $2R=320$  and 364 nm spheres, the observed lines are in the

frequency range that the present model indicates. Unfortunately, the (2,0) line, expected to be the dominant one in the  $l=0$  sequence for  $qr=5\div 6$  for both the scattering mechanisms, as shown in Figs. 2 and 5, is not detected. Its frequency is expected at about 21 GHz in the  $D=364$  nm sample (at  $\approx 15$  GHz in the  $D=515$  nm sample), just behind the range of the measurement. Only even  $l$  values are observed, whereas in the present model, odd and even  $l$  values should have comparable activities, and the (1,3) and the (1,5) would be expected to appear.

In the experiments by Cheng *et al.*, particle aggregates of polystyrene (PS) were studied. The size was in the range  $170 < 2R < 860$  nm. Vibrational modes  $(1,l)$  with  $2 < l < 7$  were observed. Higher frequency modes attributed to (2,10), (1,11), (2,13), (2,17), (1,19), (3,21), and (2,22) were also observed. No apparent rule seems to be present in the sequence of the latter set of modes, but it is possible that the assignments, based on the fit of the observed frequencies, are not correct. The most important fact is that the  $l=0$  modes are not observed. With the sound velocities of PS used in the fit ( $v_L=2350$  m/s and  $v_T=1210$  m/s), the (1,0) mode is expected at a frequency (GHz)  $f=2130/D$  (nm), the (2,0) mode at  $f=4620/D$ , and the (3,0) mode at  $f=7010/D$ . An intense peak was observed at  $f=2310/D$  (nm), attributed to the (1,5) mode and weaker peaks at  $f=4700/D$  (nm) and  $f=7450/D$  (nm), attributed to the (1,11) and (1,19) modes, respectively. Some assignments should be possibly revised, but the intensities of the Brillouin lines need to be detected as a function of the particle size. Even if the spectra are recorded in a 10° scattering angle, all  $q$  values up to the backscattering one ( $0 < q < q_{BS}=4\pi n_r/\lambda_0$ ) contribute. In fact, multiple scattering is severe in these measurements because PS has a high refractive index ( $n_r=1.59$ ). Anyway, even if  $qR$  is not well defined, its range increases as the particle size increases, and new modes appear with higher  $n$  and  $l$ . This explains the observed ‘‘cutoff’’ at a frequency  $\omega = qv_{BS}v_L$ . In fact, we have seen that only modes nearly resonant with  $qv_L$  give a strong contribution to BS. All modes with frequencies  $0 < \omega < qv_{BS}v_L$  are resonant with some  $qv_L$  value, and this explains the observed plateaux with the cutoff.

## VII. CONCLUSIONS

For spherical nanoparticles much smaller than the wavelength of the light ( $qR \ll 1$ ), the Raman active acoustic vibrations are the  $l=0$  and  $l=2$  spheroidal ones. The physical mechanism of the photon-phonon interaction depends on the system and determines the relative activity of the two sequences of vibrations. The Raman coupling coefficient, especially for the  $l=0$  vibrations, is nearly the same for all the modes of a sequence, with different radial wave vectors. However, the  $[n(\omega)+1]/\omega \sim 1/\omega^2$  factor due to the thermal averaging in harmonic approximation determines a Raman spectrum with a sequence of peaks of decreasing intensity as the radial index  $n$  increases. For this reason, only the first mode,  $n=1$ , of the  $l=0$  and/or  $l=2$  spheroidal vibrations is clearly observed in most systems.

When the size of the particles is comparable to the photon wavelength, the scenario strongly changes. A different mechanism of inelastic light scattering appears, i.e. the polarizability modulation related to density changes, which is typical of Brillouin scattering and which is negligible for small particles. Furthermore, the contribution of the polarizability modulation induced by the relative displacements of atoms, which produces the Raman scattering in small particles, strongly changes. For both mechanisms, spheroidal modes, other than those with  $l=0$  and  $l=2$ , become active. As  $qR$  increases, much higher  $l$  modes become important. At the same time, much higher  $n$  modes of the sequences become important. In relatively large particles,  $qR \gg 1$ , and for a defined  $qR$  value, the active  $(n, l, m)$  spheroidal modes are those with frequency close to that of the active acoustic modes in the bulk material, i.e.,  $\omega^{nl} \approx qv_L$ , in the case of the “Brillouin” scattering mechanism, which produces polarized scattering. The same happens for the “Raman” mechanism, but it produces also depolarized scattering of modes with  $\omega^{nl} \approx qv_T$ . The shapes of the spectra are easily predicted in the two extreme cases of  $qR \ll 1$  and  $qR \gg 1$ . The evolution of the spectra when  $qR$  varies in between is not simple. In fact, the scattered fields by the Brillouin and by the Raman mechanism have different  $qR$  dependences, and they will sum up with interferences. The relative importance of the two mechanisms also changes. For  $qR \ll 1$ , only the Raman mechanism is active, whereas for  $qR \gg 1$ , the Brillouin mechanism is expected to be dominant (in the polarized spectra) because this is the case of ordinary Brillouin scattering in glasses. Torsional modes produce only depolarized scattering from modes with  $\omega^{nl} \approx qv_T$ .

The analysis assumes that  $\mathbf{q}$  is well defined in the experiment, having excited the sphere with a plane wave and detected the scattered light at a well defined angle. This is not simple, from the experimental point of view, when dealing with spherical scatterers. If the sample is a powder, the strong elastic scattering produces multiple scattering. Any polarization information is lost, and light scattered at all  $q$  values,  $0 < q < 4\pi/\lambda$ , is collected. Even if the sample is a single sphere, the polarizations and  $\mathbf{q}$  are not precisely defined. The collected light will contain light scattered at all  $q$  values that has been reflected at the internal surface of the sphere. Furthermore, the exciting field is not a plane wave inside the sphere because of the refraction at different angles of the incoming plane wave at the sphere surface (a complete treatment should use the exciting and scattered electric fields given by the Mie theory).

Therefore, it would be important to succeed in measuring samples made by spherical particles embedded in a solid or a liquid matrix, with matched refractive index, in order to obtain polarized spectra at different well defined  $\mathbf{q}$  values.

The present results give some indication on the activity of the acoustic modes of a sphere and should help in assigning the spectra with better confidence than by fitting only the observed frequencies.

#### ACKNOWLEDGMENTS

The author acknowledges E. Duval and M. Mattarelli for useful discussions.

\*Fax: +39-0461-881696. montagna@science.unitn.it

<sup>1</sup>H. Lamb, Proc. London Math. Soc. **13**, 187 (1882).

<sup>2</sup>E. Duval, Phys. Rev. B **46**, 5795 (1992).

<sup>3</sup>M. Montagna and R. Dusi, Phys. Rev. B **52**, 10080 (1995).

<sup>4</sup>S. V. Gupalov and I. A. Merkulov, Phys. Solid State **41**, 1349 (1999).

<sup>5</sup>G. Bachelier and A. Mlayah, Phys. Rev. B **69**, 205408 (2004).

<sup>6</sup>M. Mattarelli, M. Montagna, F. Rossi, A. Chiasera, and M. Ferrari, Phys. Rev. B **74**, 153412 (2006).

<sup>7</sup>E. Duval, A. Boukenter, and B. Champagnon, Phys. Rev. Lett. **56**, 2052 (1986).

<sup>8</sup>G. Mariotto, M. Montagna, G. Vilianni, E. Duval, S. Lefrant, E. Rzepka, and C. Mai, Europhys. Lett. **6**, 239 (1988).

<sup>9</sup>M. Fujii, T. Nagareda, S. Hayashi, and K. Yamamoto, Phys. Rev. B **44**, 6243 (1991).

<sup>10</sup>R. Ceccato, R. Dal Maschio, S. Gialanella, G. Mariotto, M. Montagna, F. Rossi, M. Ferrari, K. E. Lipinska-Kalita, and Y. Ohki, J. Appl. Phys. **90**, 2522 (2001).

<sup>11</sup>Y. Jestin, N. Afify, C. Armellini, S. Berneschi, S. N. B. Bhaktha, B. Boulard, A. Chiappini, A. Chiasera, G. Dalba, C. Duverger, M. Ferrari, C. E. Goyes Lopez, M. Mattarelli, M. Montagna, E. Moser, G. Nunzi Conti, S. Pelli, G. C. Righini, and F. Rocca, Proc. SPIE **6183**, 438 (2006).

<sup>12</sup>V. K. Tikhomirov, D. Furniss, A. B. Seddon, M. Ferrari, and R. Rolli, Appl. Phys. Lett. **81**, 1937 (2002).

<sup>13</sup>M. Montagna, E. Moser, F. Visintainer, L. Zampedri, M. Ferrari, A. Martucci, M. Guglielmi, and M. Ivanda, J. Sol-Gel Sci. Technol. **26**, 241 (2003).

<sup>14</sup>M. Ivanda, K. Babocsi, C. Dem, M. Schmitt, M. Montagna, and W. Kiefer, Phys. Rev. B **67**, 235329 (2003).

<sup>15</sup>M. Ivanda, A. Hohl, M. Montagna, G. Mariotto, M. Ferrari, Z. Crnjak Orel, A. Turkovic, and K. Furic, J. Raman Spectrosc. **37**, 161 (2006).

<sup>16</sup>M. H. Kuok, H. S. Lim, S. C. Ng, N. N. Liu, and Z. K. Wang, Phys. Rev. Lett. **90**, 255502 (2003); **91**, 149901(E) (2003).

<sup>17</sup>R. S. Penciu, H. Kriegs, G. Petekidis, G. Fytas, and E. N. Economou, J. Chem. Phys. **118**, 5224 (2003).

<sup>18</sup>H. S. Lim, M. H. Kuok, S. C. Ng, and Z. K. Wang, Appl. Phys. Lett. **84**, 4182 (2004).

<sup>19</sup>W. Cheng, J. J. Wang, U. Jonas, W. Steffen, G. Fytas, R. S. Penciu, and E. N. Economou, J. Chem. Phys. **123**, 121104 (2005).

<sup>20</sup>Y. Li, H. S. Lim, S. C. Ng, Z. K. Wang, M. H. Kuok, E. Vekris, V. Kitaev, F. C. Peiris, and G. A. Ozin, Appl. Phys. Lett. **88**, 023112 (2006).

<sup>21</sup>B. J. Berne and R. Pecora, *Dynamic Light Scattering* (Wiley, New York, 1976).

<sup>22</sup>P. Benassi, O. Pilla, V. Mazzacurati, M. Montagna, G. Ruocco, and G. Signorelli, Phys. Rev. B **44**, 11734 (1991).



<sup>23</sup>A. E. H. Love, *A Treatise on the Mathematical Theory of Elasticity* (Dover, New York, 1944).

<sup>24</sup>The Brillouin spectrum contains also the peak of transverse phonons, here not considered because it is due to a different

physical mechanism, as already discussed.

<sup>25</sup>L. Saviot and D. B. Murray, *Phys. Rev. B* **72**, 205433 (2005).

<sup>26</sup>Y. Li, H. S. Lim, S. C. Ng, and M. H. Kuok, *Chem. Phys. Lett.* **440**, 321 (2007).